Wind effects on air-cooled condenser performance

LEILA BORGHEI RAMIN HAGHIGHI KHOSHKHOO
R&D department Mechanical engineering department
Monenco Iran Consultant Engineers Power and Water University of technology (PWUT)
Tehran, IRAN
Borghei.leila@yahoo.com khoshkhoo@pwut.ac.ir

Abstract: One of the most significant systems which play a crucial role in power production is the cooling systems. This paper concentrates on the effects of different wind direction and speed on the performance of a complete three-dimensional Air Cooled Condenser (ACC). The ACC model is simulated using the Fluent computational fluid dynamics (CFD) software. The hot air recirculation (HAR) is a common trouble in the air-cooled power units. HAR is affected by the arrangement of the air-cooled island, the environmental condition around the direct air-cooled system, wind direction and wind speed. In this paper, two different wind directions are considered: for case A the wind direction angle α= 90° and β=66° for case B. Results show that the plume rise angle (angle between plume and vertical) enhanced with the increase of wind speed. The hot air recirculation increases with the increment of velocity speed. Case A has a critical wind direction angle. Wind causes an air temperature increase at the fan inlet due to hot air recirculation, resulting in the deterioration of the heat transfer performance. The hot air recirculation is the main factor responsible for the reduction of heat rejection rate. The peak value of the hot air recirculation occurs at 9 m/s and wind direction angle in case A.

Key-Words: ACC, wind, speed, direction, HAR, performance

1 Introduction

Due to the serious water shortage in many countries, the most prevailing cooling systems are dry cooling systems of various types. The ACC is normally designed in the shape of an A-frame, with steam entering along the apex and considering as it passes downward through finned tubes. There is a key engineering advantage in keeping the steam duct short as possible to minimize steam pressure losses. As a result, the ACC is normally located near the turbine building itself.

In air-cooled condensers, there are many parameters that may affect their performance either slightly or heavily: The environmental wind speed, wind direction and surroundings of the ACC.

Early in the 1990s, some researchers have paid attentions on this problem. Du Toit et al. [1] concluded that the heat transfer of an ACHE should be based on local flow conditions and the influence of the flow field on fan performance and recirculation should be taken into account. The heat transfer performance of ACSCs is closely related to the thermal-flow field about and through it. Some experimental and numerical studies have been conducted for investigating the thermal flow field [2, 3–5], and it is found that computational fluid dynamics (CFD) is a very effective way to investigate the performance of ACCs [6]. Du Toit and Kro¨ger [7] and Duvenhage and Kroger [8] numerically investigated the recirculation in windless conditions and got an empirical correlation with which plume recirculation in windless conditions can be predicted for different forced draught ACHE geometries.

The effects of different fan inlet sections on the fan performance are experimentally or numerically investigated and some valuable data were obtained for optimal fan performance by some researchers (Salta and Kroger [9], Duvenhage et al. [10], Meyer [11], Hotchkiss et al. [12], Stinnes and von Backstrom, [13]). Chu [14] estimated the plume chimney height above a forced draft ACHE operating under natural convection with a derived equation and presented fan less cooling design opinion which may increase operational safety and lead to potential savings in fuel cost.

Kroger [15] found that nearby flow interaction between an air cooled heat exchanger and adjacent buildings or structures can significantly complicate flow patterns and reduce plant performance.

The principal aim is to investigate the overall flow distribution and temperature field on the air cooling condenser performance. In addition the variation of fan inlet temperature was considered under different wind speeds. In this paper, two different boundary conditions are considered: for case A, wind direction angle α=90° and the wind direction angle β=66° (prevailing wind) for case B.

2 Model Description

The south of Iran such as Abadan is poor in water. In such conditions, the air cooled heat exchangers (ACHE), in which air is used as the working medium to condense

the exhaust steam from turbine to water, is preferable to water-cooled ones in a power plant. The ACC platform is supported by 70 steel columns at an elevation of 30 m. According to the above geometry size and relative positions of power plant buildings, the basic model was set up and illustrated in Figure 1. The overall dimension of ACC is 102.6 ×75.064 ×10.5 m.

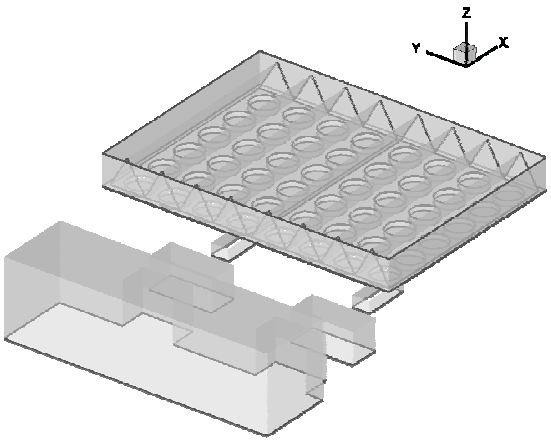

Fig. 1: plot plan of the Abadan air cooling condenser

In order to make the numerical simulation manageable, some assumptions are made as follows:

- steady-state condition
- Incompressible viscous fluids

2.1 Governing Equation

The general governing equation form is given as follows: [7]

$$\frac{\partial}{\partial x}(\rho u\phi)+\frac{\partial}{\partial y}(\rho v\phi)+\frac{\partial}{\partial z}(\rho w\phi)= \frac{\partial}{\partial x}(\Gamma_\phi\frac{\partial\phi}{\partial x})+\frac{\partial}{\partial y}(\Gamma_\phi\frac{\partial\phi}{\partial y})+\frac{\partial}{\partial z}(\Gamma_\phi\frac{\partial\phi}{\partial z})+S_\phi \quad (1)$$

Furthermore, the terms on the left side are the convection terms, and the first three terms on the right side, the diffusive terms. For continuity equation:

$$\phi=1,\Gamma_\phi=0,S_\phi=0 \quad (2)$$

x-momentum equation:

$$\phi=u,\Gamma_\phi=\mu_e \quad (3)$$

$$S_\phi=-\frac{\partial p}{\partial x}+\frac{\partial}{\partial x}(\mu_e\frac{\partial u}{\partial x})+\frac{\partial}{\partial y}(\mu_e\frac{\partial v}{\partial x})+\frac{\partial}{\partial z}(\mu_e\frac{\partial w}{\partial x})+F_x \quad (4)$$

Y-momentum equation:

$$\phi=v,\Gamma_\phi=\mu_e \quad (7)$$

$$S_\phi=-\frac{\partial p}{\partial y}+\frac{\partial}{\partial x}(\mu_e\frac{\partial u}{\partial y})+\frac{\partial}{\partial y}(\mu_e\frac{\partial v}{\partial y})+\frac{\partial}{\partial z}(\mu_e\frac{\partial w}{\partial y})+F_y \quad (8)$$

Z-momentum equation:

$$\phi=w,\Gamma_\phi=\mu_e \quad (9)$$

$$S_\phi=-\frac{\partial p}{\partial z}+\frac{\partial}{\partial x}(\mu_e\frac{\partial u}{\partial z})+\frac{\partial}{\partial y}(\mu_e\frac{\partial v}{\partial z})+\frac{\partial}{\partial z}(\mu_e\frac{\partial w}{\partial z})+F_z \quad (10)$$

The effect of the buoyancy force on the air is taken into account by means of the boussinesq model, in which the buoyancy force in the momentum equation is approximated by:

$$F_z=g(\rho-\rho_\circ) \quad (11)$$

Energy equation:

$$\phi=T,\Gamma_\phi=\frac{\mu_e}{\mathrm{Pr}} \quad (12)$$

$$S_\phi=\frac{1}{C_p}(u\frac{\partial P}{\partial x}+v\frac{\partial P}{\partial y}+w\frac{\partial P}{\partial z}+G)+F_E \quad (13)$$

The production term G in the equation for energy is defined as follows:

$$G=\mu_e\left\{2\left[(\frac{\partial u}{\partial x})^2+(\frac{\partial v}{\partial y})^2+(\frac{\partial w}{\partial z})^2\right]+(\frac{\partial v}{\partial x}+\frac{\partial u}{\partial y})^2+(\frac{\partial v}{\partial z}+\frac{\partial w}{\partial y})^2+(\frac{\partial u}{\partial z}+\frac{\partial w}{\partial x})^2\right\} \quad (14)$$

Turbulence $k-\varepsilon$ model, turbulent kinetic energy:

$$\phi=k,\Gamma_\phi=\frac{\mu_e}{\sigma_k},S_\phi=G-\rho\varepsilon \quad (15)$$

Turbulent kinetic energy dissipation rate:

$$\phi=\varepsilon,\Gamma_\phi=\frac{\mu_e}{\sigma_\varepsilon},S_\phi=\frac{\varepsilon}{k}(C_1G-C_2\rho\varepsilon) \quad (16)$$

2.2 Boundary Conditions

Figure 2 shows the computational domain with the size of 500×500×1500 m^3. At the outlet, the boundary condition was assigned as pressure outlet. No-slip and impermeable velocity condition are applied to all walls. At the inlet, a velocity inlet is expressed as follows:

$$\frac{U}{U_\infty}=(\frac{y}{y_\infty})^{0.345} \quad (18)$$

The crosswind U_∞ blows at a speed of $3\,m/s$ and y_∞ is the height of the ACC above the ground. Fan boundary is simply regarded as a uniform circular plane modeled by using a velocity inlet boundary condition. The temperature of fan boundary is 25.9°C (ambient temperature), fan diameter D=9144 mm and its volumetric flow rate is 567 m^3/s.

Figure 3 shows two different boundary conditions are

considered: for case A, wind direction angle α= 90° and the wind direction angle β= 66° (prevailing wind) for case B.

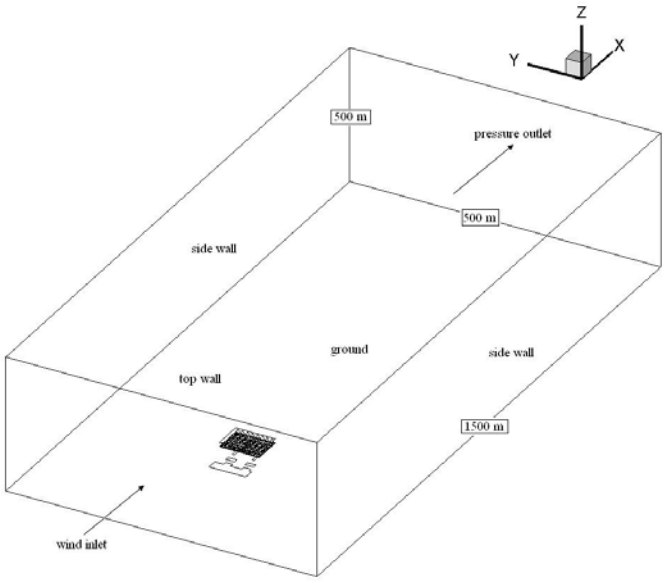

Fig. 2: the computational domain of ACC

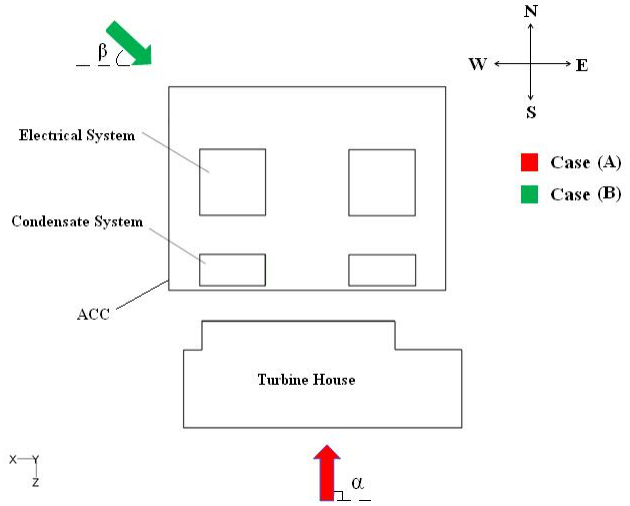

Fig. 3: up view of the system geometry with wind directions

The solution strategy is based on SIMPLE [16] algorithm and the $k-\varepsilon$ model for turbulence are employed. The first order upwind differencing scheme used to insure stability. A mesh with about 1500000 grid points was found to provide sufficient resolution. Figure 4 shows the ACC and domain grid. The solution was considered to be convergent when relative error of each dependent variable between two consecutive iterations is less than 10^{-3}.

2.3 Numerical Algorithm and methods

The solution strategy is based on SIMPLE [16] algorithm and the $k-\varepsilon$ model for turbulence are employed. The first order upwind differencing scheme used to insure stability. A mesh with about 1500000 grid points was found to provide sufficient resolution. Figure 4 shows the ACC and domain grid. The solution was considered to be convergent when relative error of each dependent variable between two consecutive iterations is less than 10^{-3}.

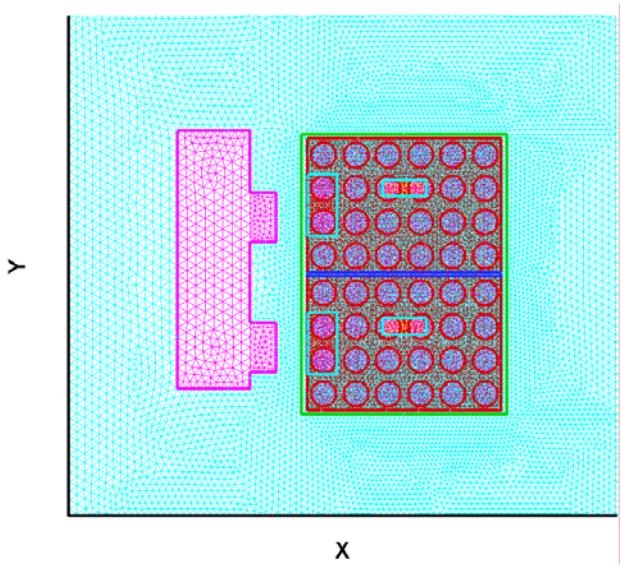

Fig. 4: grids of geometrical model

3 Results and Discussions

In this paper, the influence of some key parameters will be studied, such as wind speed, wind direction. The three-dimensional of ACC model was investigated in two different cases; Case A: the wind blows in the -z direction (the wind blows from the turbine house side) and Case B: the wind blows in the positive x-z direction (66° with the respect to the x-z direction). Three wind speeds that the velocity magnitude is 3, 6, and 9 m/s are selected, against two different wind directions.

3.1 Effect of Wind Speed on HAR

From the figures 5 and 6, it can be seen that the velocity vectors magnitude at 9 m/s is higher than 3 m/s. therefore 9 m/s is the worst velocity. Also the Hot air recirculation increases with the increment of velocity speed.

3.2 Effect of Wind Direction on HAR

In figure 7, the plume recirculation can be clearly seen around the ACC. Results show that vortex between ACC and turbine house and hot air recirculation in case A

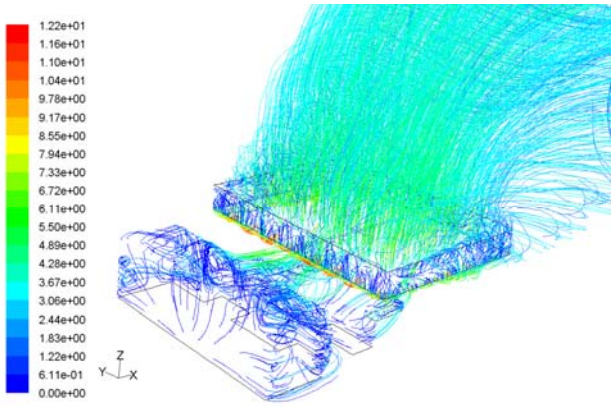

Fig. 5: Hot air recirculation at wind speed V=3 m/s in case A

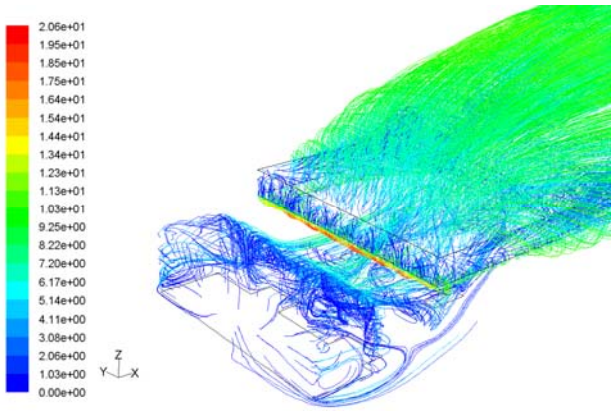

Fig. 6: Hot air recirculation at wind speed V=9 m/s in case A

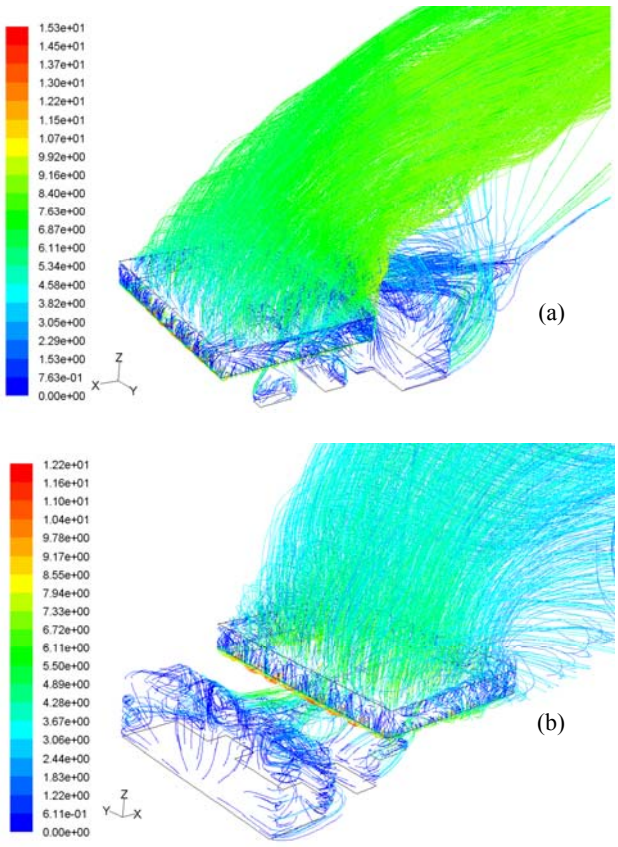

Fig. 7: Trend of hot air recirculation at wind speed V=3 m/s, case B (a) - case A (b)

higher than case B. When the steam turbine house and other buildings are upwind of the ACC, a large wake structure is formed in the area where the ACC is located. Due to the strong negative pressure field generated by the wake flow and the platform fans, some of the air exhausted from the top of the upstream portion of the platform was drawn down into the inlets of the ACC. The result is that part of the hot exhaust air from the ACC returns to the inlet region of the condensers. If a large amount hot exhaust air recirculation takes place, a significant increase in the ACC inlet air temperature will result, greatly reducing the efficiency of the ACC.

3.3 Temperature Profile and Wind Speed

Figures 8-11 show the effect of wind speed on plume rise angle (angle between plume and vertical). Temperature profiles shows that the heated air flow forms a plume rising upward after leaving from the ACC for the case of no wind, whereas it becomes a convergent taper for the case of natural wind. When the wind blows at an angle 90° (case A), the hot air exiting from ACC has been sucked to the fan platform. At the wind speed 3 m/s the plume rise angle is approximately 30°, 45° at 6 m/s and 55° at 9 m/s. therefore plume divergent increases with the increase of wind speed.

3.4 Temperature Profile and Wind Direction

Temperature profiles in figures 12-14 shows that the hot air flow leaving the ACC turns into a no divergent plume for the case of no wind, whereas it becomes a convergent taper for the case of natural wind. It can be seen that the tendency of the plume in case A affecting the fan inlet flow, but in case B the divergence of the plume is to the turbine house and may not affect the inlet flow of the fan.

3.5 Effect of Wind on Fan Inlet Temperature and Heat Rejection

Since hot air exiting from ACC flows into the fan platform from the edges, the temperature of the fan inlet will increase, this may lower the heat rejection rate of ACC. Figure 15 shows that fan inlet temperature rise in case A because of the greater HAR phenomenon, higher than case B.

Figure 16 shows that the total heat rejection rate of the air-cooled platforms decreases with increasing wind speed. We can obtained from the graphs that the recirculation of hot air is easy to be result in when wind blows from the right side of the turbine house, so the wind direction in case A, is the unfavorable wind direction.

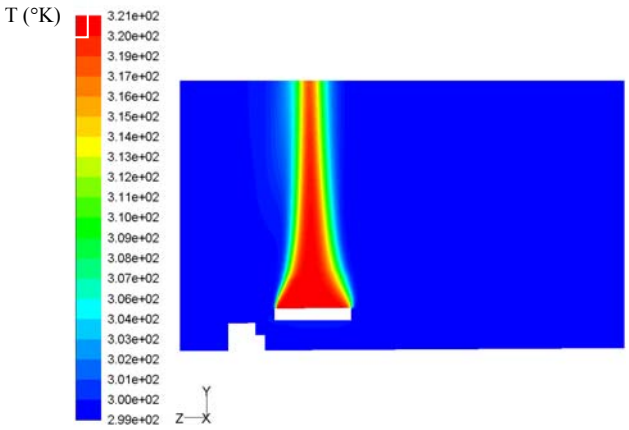

Fig. 8: temperature distribution at V=0 m/s

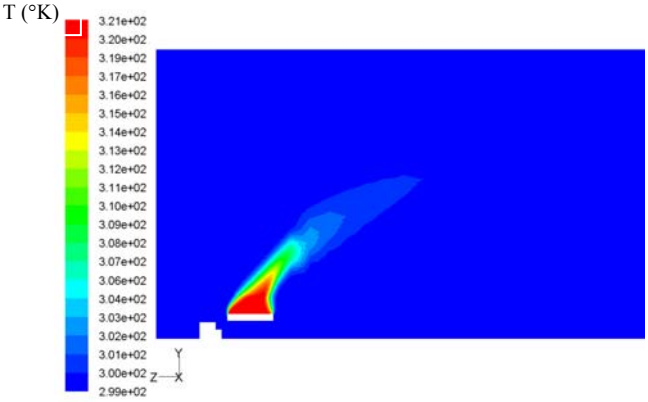

Fig. 9: temperature distribution at V=3 m/s in case A

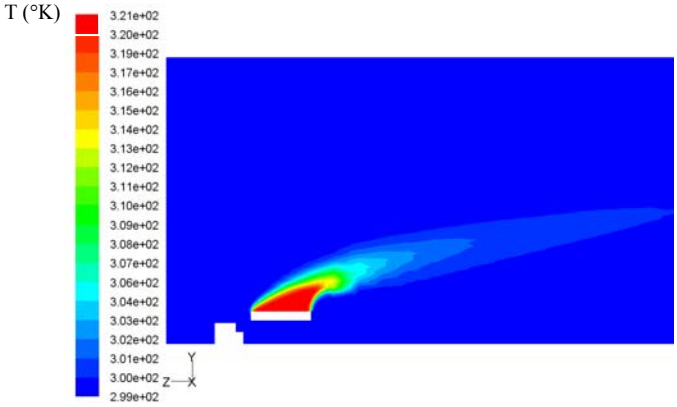

Fig. 10: temperature distribution at V=6 m/s in case A

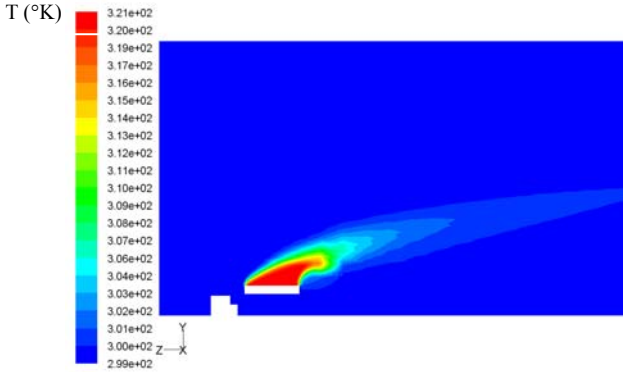

Fig. 11: temperature distribution at V=9 m/s in case A

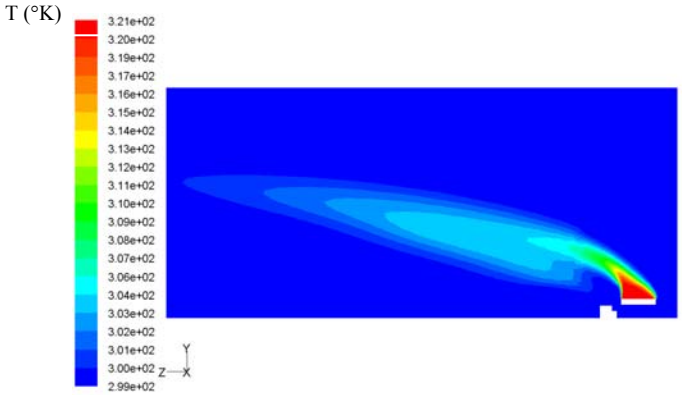

Fig. 12: temperature profile at V=3 m/s in case B

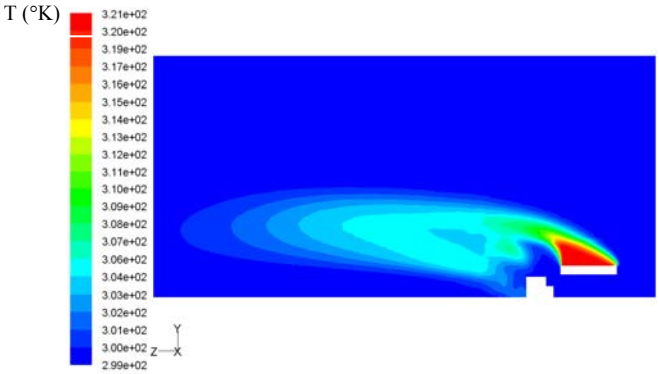

Fig. 13: temperature profile at V=6 m/s in case B

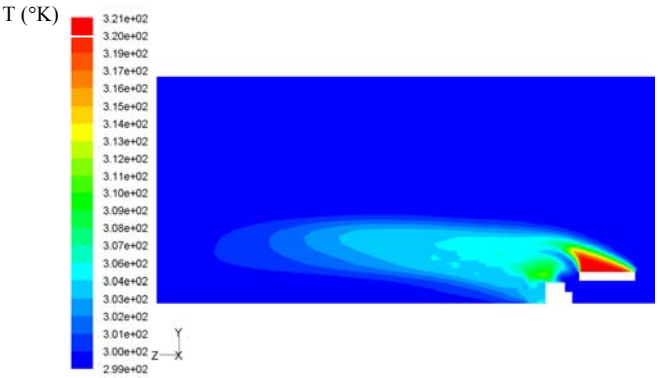

Fig. 14: temperature profile at V=9 m/s in case B

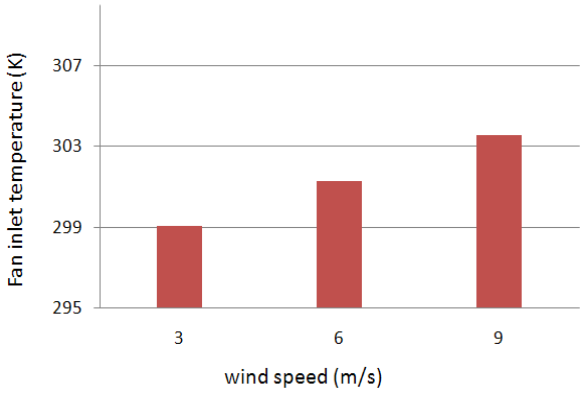

Fig. 15: effect of wind speed and direction on fan inlet temperature rise

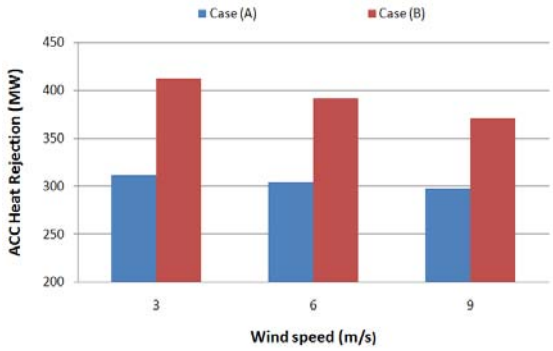

Fig. 16: heat rejection rate under different wind direction

4 Conclusion

From the results obtained in this work, the following conclusions can be derived as follows:

- When the wind comes from the side of the turbine house, the HAR is quite high.
- The Hot air recirculation increases with the increment of velocity speed.
- The peak value of the HAR occurs at 9 m/s and wind direction α=90°.
- At the wind speed 3 m/s the plume rise angle is approximately 30°, 45° at 6 m/s and 55° at 9 m/s.
- Heat rejection rate reduces with the increase of the wind speed.
- Increment of wind speed causes Fan inlet temperature rise.
- In case A, Fan inlet temperature rise and heat rejection rate decrease.
- Wind direction at α=90° and wind speed 9 m/s is the worse condition.

References:

[1] C.G. Du Toit and D.G. Kroger, Analysis of recirculation in mechanical-draught heat exchangers. *Proc. 3rd World Conf. on Exp. Heat Transfe., Fluid Mech. THermodyn.*

[2] K. Duvenhage, JA. Vermeulen, CJ. Meyer and DG. Kroger, Flow distortions at the fan inlet of forced-draught air-cooled heat exchangers. *Appl Therm Eng*, 16(8/9): 1996, pp. 741–752,.

[3] HW. Krus, JO. Haanstra, R. van der Ham and B. Wichers Schreur, Numerical simulations of wind measurements at Amsterdam Airport Schipol. *J Wind Eng Ind Aerodyn*, 91, 2003, pp. 1215–1223.

[4] WS. Zhao, M. Lei, SL. Wang, N. Cui and Y. Liu, Numerical simulation and analysis of the hot air recirculation phenomenon observed in direct air-cooled system. *Proceedings of the 3rd IEEE conference on industrial electronics and applications*, vol 1–3: 2008, pp. 1624–1628.

[5] JR. Bredell, DG. Kroger and GD. Thiart, Numerical investigation of fan performance in a forced draft air-cooled heat exchangers. *Appl Therm Eng*, 2006, pp. 846–852.

[6] JA. Van Rooyen and DG. Kroger, Performance trends of an air cooled steam condenser under windy conditions. *J Eng Gas Turbines Power*, 2008.

[7] C.G. Du Toit and D.G. Kroger, Modeling of the recirculation in mechanical draught heat exchangers. *South African Inst. of Mech. Engrs. R & DJ*, Vol. 9: 1993, pp. 2–8.

[8] K. Duvenhage and D.G. Kroger, Plume recirculation in mechanical draught heat exchangers. *Heat Transfer Eng.*, Vol. 16 No. 4: 1995, pp. 42–49.

[9] C.A. Salta and D.G. Kroger, Effect of inlet flow distortions on fan performance in forced draught air-cooled heat exchangers. *Heat Recovery Systems & CHP*, Vol. 15 No. 6: 1995, pp. 55-61.

[10] K. Duvenhageand D.G. Kroger, The influence of wind on the performance of forced draught air-cooled heat exchangers. *Journal of Wind Engineering and Industrial Aerodynamics*, Vol. 62: 1996, pp. 259-77.

[11] C.J. Meyer, Numerical investigation of the effect of inlet flow distortions on forced draught air-cooled heat exchanger performance. *Applied Thermal Engineering*, Vol. 25 Nos 11/12: 2005, pp. 1634-49.

[12] P.J. Hotchkiss, C.J. Meyer and T.W. von Backstrom, Numerical investigation into the effect of cross-flow on the performance of axial flow fans in forced draught air-cooled heat exchangers. *Applied Thermal Engineering*, Vol. 26 Nos 2/3: pp. 2-8.

[13] W.H. Stinnes and T.W. von Backstrom, Effect of cross-flow on the performance of air-cooled heat exchanger fans. *Applied Thermal Engineering*, Vol. 22 No. 12: 2002, pp. 1403-15.

[14] C.M. Chu, A preliminary method for estimating the effective plume chimney height above a forced draft air-cooled heat exchanger operating under natural convection. *Heat Transfer Engineering*, Vol. 23 No. 3: 2002, pp. 3-12.

[15] D. Kroger, Air-cooled heat exchangers and cooling towers thermal flow performance evaluation and design, *PennWell Corporation*, 2004.

[16] S. Patankar, *Numerical Heat Transfer and Fluid Flow*, Hemisphere, Washington DC. 1980.